Aerosol source apportionment around a large coal fired power plant—Thermoelectric Complex Jorge Lacerda, Santa Catarina, Brazil

Maria Luiza D.P. Godoy[a,*], José Marcus Godoy[a,b], Paulo Artaxo[c]

[a]Instituto de Radioproteção e Dosimetria, Comissão Nacional de Energia Nuclear, CP 37750, Barra da Tijuca, RJ 22642-970, Rio de Janeiro, Brazil
[b]Departamento de Química, Pontifícia Universidade Católica do Rio de Janeiro, Rua Marquês de São Vicente 225, Gávea, RJ 22453-900, Rio de Janeiro, Brazil
[c]Instituto de Física, Universidade de São Paulo, Rua do Matão, Travessa R, 187, CEP 05508-900, São Paulo, Brazil

Abstract

The Thermoelectric Complex Jorge Lacerda (TCJL) is located in the Southern part of Brazil, at the community of Capivari de Baixo, in the state of Santa Catarina, 130 km from Florianópolis. The TCJL is the largest coal burning thermoelectric complex of Latin America, formed by seven power plants and with a total capacity of 832 MW. Two aerosol-sampling campaigns were performed, during summer and winter seasons, in 12 different sites around the TCJL with aerosol collection for 10 sampling days each site. Stacked filter units were used to collect fine and coarse aerosol particles and trace element analysis by inductively coupled plasma–mass spectrometry(ICP-MS) was performed in both size fractions. Gravimetric analysis and reflectance measurements provided aerosol mass and black carbon concentrations. Very good detection limits for up to 42 elements were obtained. Receptors models such as principal factor analysis, cluster analysis and absolute principal factor analysis were applied in order to identify and quantify the aerosol particle sources. Emissions from the TCJL are the main source of elements such as As, Bi, Cd, Pb, Sb and Se in both aerosol fractions, ranging from 34% up to 83% in mass. Based on absolute principal component analysis, source profiles were calculated. These profiles were compared with those observed on the EPA Speciate 3.1 data bank and a good similarity was observed. The ICP-MS analysis of trace elements in aerosols has proven to be reliable and feasible for large amount of samples, and the coupling with receptor models provided an excellent method for quantitative aerosol source apportionment in industrial complexes.
© 2005 Elsevier Ltd. All rights reserved.

Keywords: ICP-MS; Aerosol analysis; Coal power plant; Receptor model; Trace elements; Brazil

1. Introduction

The Thermoelectric Complex Jorge Lacerda (TCJL) is located in the community of Capivari de Baixo, in the Southeast area of the state of Santa Catarina, 130 km from Florianópolis, the state capital. The TCJL is the

*Corresponding author. Tel:/fax: +0055 21 2442 2861.
E-mail address: malu@ird.gov.br (M.L.D.P. Godoy).

largest coal burning thermoelectric complex of Latin America, formed by seven power plants and with a total capacity of 832 MW and consumes about 2.9×10^6 tons of coal per year (Japan International Cooperation Agency—JICA, 1997). Flat lands of recent sedimentary formation with average height of 9 m above sea level dominate the area around the complex, occupied by rice plantations. The complex is located between two cities, Capivari de Baixo and Tubarão. The main rivers of the area are the Tubarão and Capivari. An aerial view from the TCJL and its environment is shown in Fig. 1. The average wind speed is $2\,\mathrm{m\,s^{-1}}$ and its direction distribution is quite homogeneous, furthermore, with a calm frequency of 11.5%. The meteorological conditions at Jorge Lacerda with weak winds and high frequency of stable conditions tend to produce air pollution episodes in the region (Japan International Cooperation Agency—JICA, 1997).

All the power plant units of TCJL have electrostatic precipitators with an efficiency of approximately 98%, which remove particulates in suspension in the gaseous effluent. To help the atmospheric pollutants dispersion,

Fig. 1. Aerial photograph of the Thermoelectric Complex Jorge Lacerda (TCJL) and its surroundings.

the 4 older generating units are equipped with a 150 m height chimney. Each 125 MW unit has a 100 m chimney, and the newest unit of 350 MW has a 200 m chimney. The area is monitored by the power plant operator, with the help of SO_2 and NO_x automatic monitoring stations and manual total suspended particulates (TSP) sampling. No environmental data or measurements concerning trace element concentrations are available for the site (Japan International Cooperation Agency—JICA, 1997).

The objective of this work was to investigate the atmospheric impact of the industrial complex in the region air quality. Additionally, we would like to learn if the use of advanced trace element analysis, (inductively coupled plasma mass spectrometry—ICP-MS) with the measurements of a high number of trace elements and use of multiple receptor models could be used to quantitatively investigate the impact of the industrial complex. Stacked filter units (SFU) were used to collect fine and coarse aerosol particles and trace element analysis by ICP-MS was performed in both size fractions. Receptors models such as principal factor analysis, cluster analysis and absolute principal factor analysis were applied in order to identify and quantify the aerosol particle sources. The obtained results should help to verify the actual contribution of the TCJL to the local and regional atmospheric aerosol loading, with reference to the mass concentration of fine and coarse mode aerosols, of black carbon and of trace elements.

2. Material and methods

Two aerosol-sampling campaigns were performed at twelve sites (Fig. 2), in the summer 1999 and the winter 2000, during 10 days with 24 h sampling time. In order to choose the sampling points, it was taking into account the existence of two urban areas nearby, Capivari de Baixo and Tubarão, as well as the predicted dispersion pattern at distances up to 5 km. Additionally, the sampling points should be feasible in terms of local logistics, located far from trees, roads or any other obstacles, with power supply available, safe of intrusion and with grass covered soil.

The aerosol particles were collected using the SFU (Artaxo et al., 1999; Hopke et al., 1997; Maenhaut et al., 1993), which uses an inlet providing a 50% cutoff diameter at 10-μm. The SFU collects coarse mode particles ($2.0 < dp < 10\,\mu m$) on a 47-mm diameter, 8-μm pore size Nuclepore filter while a 0.4 μm pore size Nuclepore filter collects the fine mode particles ($dp < 2.0\,\mu m$). The sum of both size fractions provides PM_{10} that refers to aerosol particles smaller than 10-μm aerodynamic diameter. The flow rate was typically 17 L min^{-1}. Particle bounce at the inlet was minimized by coating the pre-impaction plate with a thin layer of

Apiezon vacuum grease (AP 101). The sample volume was obtained with gas volume meters, calibrated with a primary standard airflow calibrator, "Gilibrator" (Gilian Instruments Corporation).

The aerosol mass concentration was obtained through gravimetric analysis using a electronic micro balance with 1 μg sensitivity (Mettler MT5). The detection limit for aerosol mass concentration is about $0.3\,\mu g\,m^{-3}$, while precision is estimated to be 10%. Black carbon (BC) concentration in the fine mode was measured using a reflectance technique (smoke stain reflectometer, Diffusion System, model M43D), calibrated using BC gravimetric standards. Elemental concentrations on the
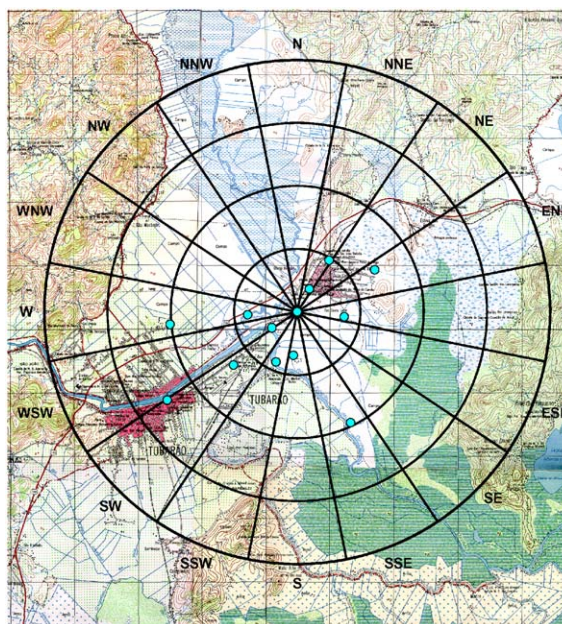
Fig. 2. Aerosol sampling sites used in this study, with the TCJL at the center (radius at 2, 4, 6 and 8 km from the TCJL).

Table 1
Achieved elemental detection limits in aerosol

Detection limit range (ng m^{-3})	Elements
<0.01	Sm, U, Eu, Cs, Dy, Be, Pr, Gd, Bi, Th, Y, Nd, Ga, La, As, Li, W, Cd, Rb, Sb, Ge, Co
0.01–0.1	Ag, Ce, Nb, Mo, Se, Sr, Mn, Ba, V
0.1–1	Pb, Ni, Sc, Cu, Cr
1–10	K, Zn, Na, Mg, Fe, Al, Ti

Table 2
Average aerosol mass concentration measured in the different sampling points, as well as black carbon concentration

Sampling site	Summer 1999				Winter 2000			
	IPM ($\mu g\,m^{-3}$)	CPM ($\mu g\,m^{-3}$)	FPM ($\mu g\,m^{-3}$)	BC ($\mu g\,m^{-3}$)	IPM ($\mu g\,m^{-3}$)	CPM ($\mu g\,m^{-3}$)	FPM ($\mu g\,m^{-3}$)	BC ($\mu g\,m^{-3}$)
1	44.20	34.60	9.60	1.11	33.86	24.14	9.72	1.83
2	30.84	24.90	5.94	0.45	23.00	14.44	8.56	1.18
3	26.85	21.40	5.44	0.39	27.06	19.28	7.78	1.03
4	29.57	22.31	7.26	0.59	28.40	19.65	8.75	1.38
5	28.47	21.84	6.63	0.47	25.04	16.92	8.12	1.22
6	45.19	36.12	9.07	1.40	32.32	22.70	9.62	1.93
7	41.17	32.99	8.18	0.97	30.93	22.74	8.19	1.50
8	35.98	27.47	8.51	0.89	37.64	29.29	8.35	1.67
9	28.02	22.26	5.77	0.44	19.85	12.62	7.23	1.06
10	40.03	31.60	8.43	1.03	30.80	22.87	7.93	1.38
11	34.76	28.26	6.50	0.79	24.74	16.47	8.27	1.28
12	26.47	21.04	5.44	0.28	23.97	16.83	7.14	1.02

IPM——inhalabe particle mass concentration (PM_{10}), equal to FPM + CPM; CPM——coarse mode aerosol mass concentration, particles with diameter between $10\,\mu m$ and $2\,\mu m$; FPM——fine mode aerosol mass concentration, particles with diameter smaller than $2\,\mu m$; BC——black carbon in the fine mode.

Table 3
Elemental concentration observed in the fine and coarse particles

	Fine particles fraction				Coarse particle fraction		
	Number samples	Mean ($ng\,m^{-3}$)	SD ($ng\,m^{-3}$)		Number samples	Mean ($ng\,m^{-3}$)	SD ($ng\,m^{-3}$)
(a) *Summer sampling campaign*							
Li	104	0.11	0.15	Li	115	0.65	0.63
				Be	114	0.065	0.06
Na	105	217	66.4	Na	115	1075	307
Mg	105	38.1	10.7	Mg	115	207	60.6
Al	105	134	144	Al	115	926	807
K	105	99.2	67.0	K	115	267	165
				Ti	112	52.8	47.7
V	105	0.61	0.55	V	115	1.72	1.79
Mn	105	0.97	0.75	Mn	115	5.38	4.02
Fe	105	56.5	53.9	Fe	115	325	256
Co	102	0.044	0.052	Co	115	0.19	0.25
Cu	104	0.44	0.39				
Zn	104	5.38	3.92	Zn	115	7.24	4.77
Ga	105	0.11	0.15	Ga	115	0.49	0.51
Ge	101	0.092	0.13	Ge	115	0.28	0.31
As	105	0.28	0.28	As	115	0.49	0.63
Se	105	0.55	0.62	Se	115	0.27	0.26
Rb	105	0.65	0.48	Rb	115	1.92	1.44
Sr	105	0.51	0.28	Sr	115	2.38	1.18
Y	105	0.11	0.11	Y	115	0.63	0.51
Nb	100	0.053	0.049	Nb	115	0.31	0.26
Cd	105	0.047	0.034	Cd	113	0.027	0.10
Sb	105	0.10	0.074	Sb	115	0.054	0.047
Cs	105	0.030	0.034	Cs	115	0.16	0.16
Ba	105	2.12	1.74	Ba	115	7.04	5.43
La	105	0.16	0.15	La	115	0.91	0.70
Ce	105	0.30	0.29	Ce	115	1.68	1.32
Pr	105	0.038	0.035	Pr	115	0.22	0.17
Nd	105	0.13	0.13	Nd	115	0.78	0.61
Sm	105	0.026	0.025	Sm	115	0.15	0.12
				Eu	115	0.025	0.021

Table 3 (*continued*)

	Fine particles fraction				Coarse particle fraction		
	Number samples	Mean (ng m^{-3})	SD (ng m^{-3})		Number samples	Mean (ng m^{-3})	SD (ng m^{-3})
Gd	105	0.027	0.026	Gd	115	0.16	0.12
Dy	104	0.020	0.020	Dy	115	0.12	0.095
				W	113	0.065	0.087
Pb	105	1.29	0.81	Pb	115	1.44	1.15
Bi	105	0.020	0.022				
Th	105	0.067	0.063	Th	115	0.41	0.32
U	104	0.029	0.035	U	115	0.14	0.12
FPM*	105	7.30	2.45	CPM*	115	26.9	9.82
BC*	105	0.74	0.44				
(b) *Winter sampling campaign*							
Li	111	0.10	0.073	Li	113	0.66	0.40
Be	111	0.009	0.008	Be	113	0.063	0.042
Na	111	147	83.8	Na	113	738	417
Mg	111	50.0	31.6	Mg	113	186	74.1
Al	111	112	75.9	Al	113	1032	634
K	111	172	93.8	K	113	359	212
				Sc	113	0.33	0.16
Ti	107	8.21	5.70	Ti	113	63.2	36.7
V	107	0.63	0.46	V	113	1.63	1.08
Mn	111	1.79	0.98	Mn	113	9.96	5.96
Fe	111	58.7	30.0	Fe	113	431	252
Co	110	0.060	0.084	Co	113	0.24	0.17
				Ni	113	0.64	0.9
Cu	106	1.22	1.59	Cu	113	1.56	1.25
Zn	110	34.2	31.8	Zn	113	20.9	15.6
Ga	111	0.11	0.085	Ga	113	0.47	0.29
Ge	111	0.075	0.063	Ge	113	0.22	0.15
As	111	0.52	0.33	As	113	0.45	0.38
Se	111	0.54	0.45	Se	113	0.29	0.33
Rb	111	1.06	0.58	Rb	113	2.82	1.89
Sr	111	0.40	0.19	Sr	113	2.71	1.23
Y	111	0.10	0.070	Y	113	0.81	0.50
Nb	109	0.052	0.033	Nb	113	0.40	0.26
				Mo	113	0.10	0.083
				Ag	113	0.046	0.044
Cd	111	0.19	0.36	Cd	113	0.084	0.11
Sb	111	0.47	0.96	Sb	113	0.21	0.26
Cs	111	0.036	0.020	Cs	113	0.16	0.10
Ba	111	2.24	1.51	Ba	113	10.5	7.18
La	111	0.16	0.090	La	113	1.21	0.74
Ce	111	0.29	0.17	Ce	113	2.16	1.31
Pr	111	0.037	0.021	Pr	113	0.29	0.18
Nd	111	0.13	0.077	Nd	113	1.04	0.66
Sm	111	0.025	0.015	Sm	113	0.20	0.13
				Eu	113	0.031	0.018
Gd	111	0.025	0.016	Gd	113	0.20	0.13
Dy	111	0.018	0.012	Dy	113	0.14	0.090
W	108	0.024	0.042	W	113	0.10	0.12
Pb	111	5.74	3.61	Pb	113	3.92	4.31
Bi	111	0.053	0.049	Bi	113	0.043	0.050
Th	111	0.066	0.042	Th	113	0.55	0.40
U	111	0.031	0.032	U	113	0.18	0.13
MPF*	111	8.31	4.48	MPG*	113	19.5	9.96
BC*	111	1.34	0.94				

*Values as μg m^{-3}.

Nuclepore filters were determined using the ICP-MS technique, after total chemical dissolution applying high-purity HNO_3 and HF. Filter dissolution was performed by microwave heating in closed Teflon® vessels (microwave oven CEM MARS 5). After boric acid addition to eliminate HF excess, the solution was evaporated to the dryness under vacuum also by microwave heating and the residue was dissolved with 10 mL 2% HNO_3.

Mass spectrometric analysis was performed in a Perkin-Elmer ELAN 6000 ICP-MS instrument, with operational conditions and mass calibration similar to those described by Godoy et al. (2001). In order to improve accuracy and precision, it was chosen to run the system in the fully quantitative method, using In and Tl as internal standards. The concentrations of up to 42 elements (Li, Be, Na, Mg, Al, K, Sc, Ti, V, Mn, Fe, Co, Ni, Cu, Zn, Ga, Ge, As, Se, Rb, Sr, Y, Nb, Mo, Ag, Cd, Sb, Cs, Ba, La, Ce, Pr, Nd, Sm, Eu, Gd, Dy, W, Pb, Bi, Th and U) were determined. Typical detection limits are shown in Table 1. Reference materials, NIST SRM-3082a (air filter) and IAEA-356 (lake sediment), were used to check the analytical procedure applied, including the sample dissolution and the ICP-MS analysis. The precision of the elemental concentration measurements is in the range of 10%.

Histograms, normal and lognormal distributions were generated to validate the data and to remove outliers.

Table 4
Comparison between the observed black carbon, mass and elemental concentration on the fine and coarse particles fraction and results obtained by other authors, using the same sampling technique (values in $ng\,m^{-3}$)

	This work		São Paulo (Brazil)[a]	Birmingham (UK)[b]	Coimbra (Portugal)[b]	Brisbane (Australia)[c]	Ho Chi Minh (Vietnam)[d]	Lund (Sweden)[e]
	1999	2000						
Fine fraction								
Na	217	147		348	360	280	196	
K	99	172	407	127	320	111	832	108
Ti		8.2	31	4.7		6	101	
V	0.61	0.63	12	5.0	12		7.8	
Mn	0.97	1.8	13	9.9	14	4	14	3.4
Fe	57	59	532	114	190	50	261	52
Cu	0.44	1.2	19	30	22		1.5	1.7
Zn	5.4	34	126	297	50	27	245	18
As	0.28	0.52		4.2	1.9		2.5	
Se	0.55	0.54	3.0	2.0	0.57		0.77	1.3
Pb	1.3	5.7	42	74	250	51	79	14
BC[f]	0.74	1.3	7.6		3.1	1.8		
Mass[f]	7.3	8.3	30		30	7.3	16	
Coarse fraction								
Na	1075	738		698	1130	900	861	
K	267	359	486	71.5	190	121	1756	116
Ti	52.8	63.2	217	11.9		33	374	20
V	1.7	1.6	13	2.4	3.9		12	
Mn	5.4	10.0	32	6.4	8.7	4	52	5.0
Fe	325	431	1981	187	340	200	1222	181
Cu		1.6	44	8.5	17.8		2.8	2.9
Zn	7.2	20.9	189	55.6	20.0	9	326	10.5
As	0.49	0.45		1.5	0.45		3.6	
Se	0.27	0.29	3.0	1.1	0.22		0.75	
Pb	1.4	3.9	38	17.1	60.0	11	73	6.1
Mass[f]	26.9	19.5	46		22.5	10.4	31.8	

[a]Castanho (1999).
[b]Harrison et al. (1997).
[c]Chan et al. (1999).
[d]Hien et al. (2001).
[e]Swietlicki et al. (1996).
[f]Values in $\mu g\,m^{-3}$.

For each element, a stepwise linear regression was performed on the validated data set to analyze outliers that were above 3 standard deviations. Those elements that could not be significantly predicted by any other element were excluded from the data set. In general, were those with most of the results below or close to the quantification limit, such as W and Ti. Some samples were also excluded from the data set due to equipment failure or unusual activities, such as vegetation burning, close to the sampler. After the data validation, 105–115 samples and 34–42 elements were included on each data set (fine and coarse mode aerosol, summer and winter campaign).

In order to identify and evaluate the contribution of the pollutant sources in the fine and coarse particle fractions surrounding the TJCL, receptors models were

used (Hopke, 1999). A multivariate statistical approach was applied including principal factor analysis (PFA), absolute principal factor analysis (APFA) and hierarchical cluster analysis (Artaxo et al., 1999, Johnson and Wichern, 1998; Legendre and Legendre, 1998). All the statistical analyses were performed using the Statistical Program for Social Science (SPSS)® version 9.0.

3. Results and discussion

The average aerosol mass concentration measured in each sampling site, and sampling year, is shown in Table 2, as well as the black carbon mass concentration (BC). In general, the observed fine particles mass concentration (FPM), coarse particles mass concentration (CPM) and inhalable particles mass concentration (IPM) were quite constant between the different sampling sites during both sampling campaigns, showing strong similarity between the sampling sites. This similarity can be due to the fact that the distribution of the frequency of wind direction is quite homogeneous and the sampling region was relatively small. Therefore, all the sampling sites seem to have similar aerosol impacts. In many cases, the FPM during the winter/2000 were

Table 5
Calculated enrichment factor (EF) for fine and coarse mode aerosols

| Element	EF-PM$_{2.0}$		EF-PM$_{2.0-10}$	
	1999	2000	1999	2000
Na	**21.7**	**14.6**	**18.6**	**9.7**
Mg	**5.0**	**6.5**	4.7	3.2
Al	2.3	1.9	2.7	2.3
K	1.9	3.2	0.9	0.9
Ti		0.7	0.8	0.7
V	3.4	3.5	1.7	1.2
Mn	0.9	1.7	0.9	1.3
Co	2.1	2.9	1.6	1.5
Zn	**24.5**	**155.0**	**5.7**	**12.5**
Ga	2.9	2.7	2.2	1.5
Ge	**21.8**	**17.6**	**11.3**	**6.8**
As	**30.8**	**56.1**	**9.2**	**6.3**
Se	**90.7**	**88.6**	**7.9**	**6.3**
Rb	2.2	3.5	1.1	1.2
Sr	3.1	2.5	2.5	2.2
Y	3.0	2.8	2.9	2.9
Nb	1.1	1.1	1.2	1.1
Cd	**130.0**	**523.3**	**12.9**	**30.5**
Sb	**111.5**	**512.7**	**10.4**	**30.2**
Cs	2.4	2.8	2.2	1.7
Ba	2.9	3.0	1.6	1.8
La	3.3	3.3	3.2	3.3
Ce	2.6	2.5	2.5	2.4
Pr	3.0	2.9	3.0	3.1
Nd	2.9	2.8	3.0	3.0
Sm	2.8	2.6	2.8	2.8
Eu			2.4	2.2
Gd	2.7	2.5	2.7	2.6
Dy	2.4	2.1	2.4	2.2
W		**6.7**	3.1	3.6
Pb	**16.7**	**74.2**	3.2	**6.7**
Bi	**24.2**	**63.1**		**6.9**
Th	2.0	2.0	2.1	2.2
U	2.6	2.8	2.2	2.1

(a)

(b)

Fig. 3. Variability of the FPM and CPM concentrations with distance from the industrial complex at (a) summer 1999 and (b) winter 2000 sampling campaigns.
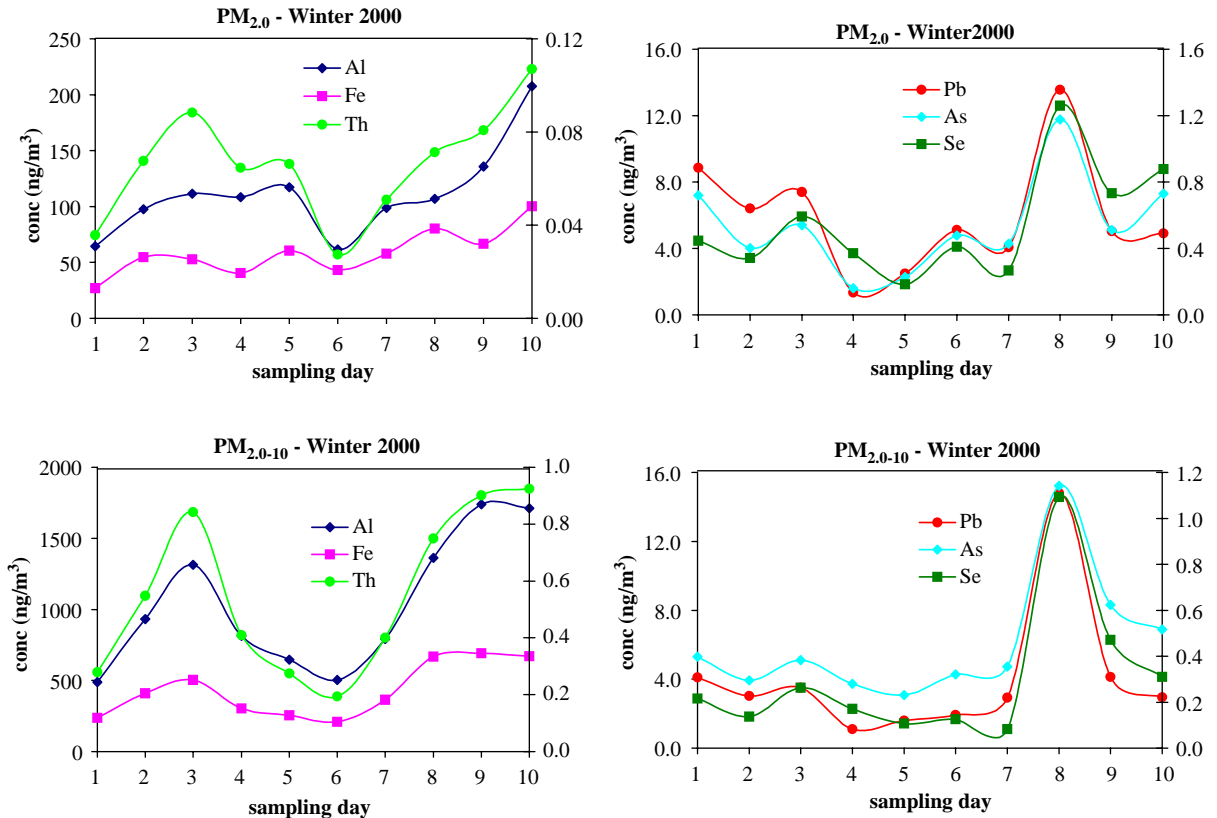
Fig. 4. Time series of the elemental concentration observed during the winter 2000 sampling campaign.

higher than during the summer/1999, as well as the BC concentration, probably because the winter session is dryer than the summer with consequent poor vegetation coverage and frequent regional biomass burning emissions. BC concentration is about 13% of the FPM that is characteristic of power plant emissions with similar particulate emission controls.

Not all the 42 elements determined by ICP-MS were observed above the detection limit in every filter of all sampling points. Also, some of the measured values did not passed after the validation procedure described on the Material and methods section. Therefore, the number of results per element per sampling campaign was always lower than 120. Table 3 shows the mean elemental concentration observed in the fine and in the coarse particles fractions during the 1999 and 2000 sampling campaigns.

By converting concentration values from elements to possible chemical components, the overall contribution of measured components to the average mass can be estimated as 20–25% in both size fractions. The mass contribution of silicon oxide can be estimated ranging from 9.6% (year 2000 fine mode) up to 37.7% (year

2000 coarse mode) assuming a Si/Al ratio similar to the average crust composition (Hien et al., 1999). Using this estimative, the percentage of the total mass evaluated reaches 37% of the $PM_{2.0}$ fraction for both sampling campaign and 44% and 63% of the $PM_{2.0-10}$ fraction in the 1999 and 2000 sampling campaign, respectively. The remaining $PM_{2.0}$ and $PM_{2.0-10}$ mass should be made up mainly of ammonium, sulphate, nitrate, water and organics, which were not measured in this work.

Comparing the mean elemental concentration in the fine and coarse particle fraction, it can be observed that Se, Sb and Cd are higher in the fine particles during both sampling campaigns, and As, Zn, Bi and Pb only during the 2000 campaign. All other elements were higher in the coarse fraction. Fine particles are largely formed on high temperature process such as the coal combustion. Therefore, volatile elements concentrated on the fly ash, such as As, Cd, Pb, Sb and Se are supposed to be found on the fine mode fraction (Godoy et al., 2001).

The FPM was slightly higher in the 2000 campaign than in 1999, however, this difference was much higher for elements that could be interpreted as originated from the TCJL. These elements includes Zn, As, Cd, Sb, Pb

Table 6
Varimax rotated factor loading matrix for fine particles in 1999

Element	Factor 1 Soil ressuspension	Factor 2 TCJL emission	Factor 3 Biomass burning	Factor 4 Sea spray	Communality
Al	**0.96**	0.22	—	—	0.98
Y	**0.96**	0.25	0.10	—	0.99
Gd	**0.95**	0.26	0.10	—	0.99
Cs	**0.95**	0.12	0.23	—	0.97
Sm	**0.95**	0.27	0.10	—	0.98
Ce	**0.94**	0.28	0.11	—	0.99
Nd	**0.94**	0.29	0.11	—	0.98
Ga	**0.94**	0.10	0.19	—	0.93
Fe	**0.94**	0.28	0.15	—	0.98
La	**0.94**	0.30	0.12	—	0.98
Pr	**0.93**	0.29	0.13	—	0.97
Th	**0.90**	0.32	—	—	0.93
V	**0.90**	0.20	0.20	—	0.89
Sr	**0.87**	0.19	0.26	0.24	0.92
Ba	**0.83**	0.18	0.30	—	0.81
As	**0.82**	—	0.29	—	0.77
Bi	**0.70**	**0.45**	0.13	—	0.71
Mn	**0.58**	**0.52**	0.38	—	0.76
Cd	0.20	**0.84**	0.26	—	0.81
Sb	0.27	**0.82**	—	—	0.75
Pb	0.39	**0.75**	0.28	—	0.79
FPM	0.46	**0.54**	0.34	0.45	0.82
K	0.17	0.17	**0.93**	0.12	0.95
Rb	0.25	0.18	**0.92**	—	0.94
BC	0.15	0.42	**0.64**	0.13	0.63
Na	−0.24	−0.11	—	**0.96**	0.98
Mg	0.21	—	0.26	**0.92**	0.96
Eigenvalue	**15.1**	**3.8**	**3.1**	**2.1**	Total variance
Variance (%)	**56.0**	**14.3**	**11.5**	**7.7**	**89.4**

and Bi, with up to 4 times higher concentrations in 2000 than in 1999, and for elements coming from biomass burning as K, Rb and black carbon, up to twice higher in 2000 than in 1999. As the 2000 sampling campaign has occurred during the wintertime, while the 1999 it was carried out during the summer period, this can be originated by less favorable dispersion conditions during the winter, associated with a larger impact of biomass burning emissions on this traditionally dry period.

The same comparison can be done for the CPM and similar results were observed, but with smaller intensity than observed on the FPM. For elements such as Sb, Cd and Pb, an increment of 3 times was observed in 2000 when compared to 1999 and of 34% for K and 47% for Rb. As the winter session is drier than the summer, during this period particles from soil ressuspension have a higher impact on the coarse mode aerosol, and also it was observed higher concentration of typical soil elements as thorium and iron in the coarse mode.

As observed on Table 4, the average CPM, FPM and BC observed in this study are lower than most urban areas. Similarly, the elemental mass concentration during both sampling campaigns are, in general, equivalent or smaller than the obtained by other authors, using the same sampling technique. Crustal elements in the coarse fraction are a consequence of the intense agricultural activities in this region. The obtained values in the fine fraction for elements such as Pb and V, normally associated to the vehicular traffic, are the smallest observed in Table 4 due to the small size of Capivari de Baixo and Tubarão urban areas.

In order to analyze ratios between the elements and possible sources, enrichment factors (EF) were calculated using a double ratio between the elemental concentration of one element normalized to iron in the aerosol and in the soil. Several elements have been proposed for this purpose as Al, Ce, Ba and Fe (Hien et al., 2001; Horton et al., 1977; Johansson et al., 1974;

Table 7
Varimax rotated factor loading matrix—fine particles 2000

Element	Factor 1 Soil ressuspension	Factor 2 Biomass burning	Factor 3 TCJL emission	Factor 4 Sea spray	Communality
U	**0.97**	—	0.15	—	0.97
Be	**0.95**	0.13	0.18	—	0.96
Li	**0.93**	0.14	0.26	—	0.96
Dy	**0.93**	0.34	—	—	0.98
Y	**0.93**	0.34	—	—	0.98
Gd	**0.89**	**0.42**	—	—	0.97
Al	**0.89**	**0.41**	—	—	0.96
Ga	**0.88**	—	0.29	—	0.86
Sm	**0.86**	**0.47**	—	—	0.97
Ge	**0.84**	—	**0.40**	—	0.87
Ce	**0.84**	**0.47**	—	—	0.94
Nd	**0.84**	**0.49**	—	—	0.96
Pr	**0.82**	**0.50**	—	—	0.94
La	**0.82**	**0.51**	—	—	0.93
Th	**0.82**	**0.47**	—	0.11	0.89
Cs	**0.78**	0.32	**0.49**	—	0.96
Sr	**0.71**	0.26	0.13	**0.56**	0.89
Fe	**0.57**	**0.76**	0.14	—	0.93
K	0.31	**0.75**	**0.46**	—	0.88
FPM	0.23	**0.74**	**0.41**	—	0.77
Rb	0.32	**0.72**	**0.50**	—	0.88
BC	—	**0.69**	**0.63**	−0.25	0.93
Mn	**0.44**	**0.65**	0.36	−0.12	0.77
Ba	**0.54**	**0.58**	0.26	—	0.70
As	0.20	0.23	**0.88**	0.19	0.91
Bi	—	0.17	**0.86**	−0.21	0.81
Se	**0.41**	0.25	**0.78**	—	0.84
Pb	—	0.18	**0.76**	0.31	0.70
Na	0.12	−0.18	—	**0.94**	0.94
Eigenvalue	**14.1**	**5.9**	**4.6**	**1.5**	Total variance
Variance (%)	**48.5**	**20.2**	**15.8**	**5.3**	**89.8**

Klein et al., 1975; Lindberg et al., 1975; Zoller et al., 1974). The elemental concentrations in the soil were obtained trough analysis performed by Godoy et al. (2004). The calculated EF values are shown on Table 5. Based on the enrichment factor values for the rare earth elements, between 2 and 3, it was taken as enriched on the aerosol phase those elements with EF higher than 4. The elements with a high enrichment factor on the fly ashes measured at this plant, such as Sb, Cd, Se, As and Pb (Godoy et al., 2001) also appears with an elevated EF on the aerosol phase, in particular on the fine particles. This can be taken as an indicative of the TCJL influence on the aerosol elemental composition around the complex.

In order to obtain a measure of the influence of the industrial complex on aerosol concentration, relationships between the FPM, CPM and the elemental concentration on both fractions with the distance to the TCJL were investigated. Fig. 3 shows this pattern for the FPM and CPM for each sampling point during both campaigns. A point represents the mean value obtained during a sampling period. No values above the Brazilian PM_{10} standards ($50\,\mu g\,m^{-3}$) or the EPA $PM_{2.5}$ standards ($15\,\mu g\,m^{-3}$) were observed. The first peak observed in Fig. 3 was attributed to resuspension of the coal and ashes deposits around the complex. The second peak is consistent with the distance of maximum impact due to the particulate matter discharged by the TCJL predicted based on a Gaussian dispersion model (Godoy, 2001). The city of Tubarão is located circa of 4 km from the TCJL and can be the reason of the observed increase in aerosol concentrations after this distance. Similar results were obtained for the elemental concentrations. The observed patterns were always the same independent of element, aerosol fraction and sampling campaign and were consistent with the FPM and CPM pattern.

Table 8
Varimax rotated factor loading matrix for coarse particles 1999

Element	Factor 1 Soil ressuspension	Factor 2 TCJL emission and road dust	Factor 3 Sea spray	Communality
Mn	**0.94**	0.16	0.17	0.94
Th	**0.92**	0.32	0.14	0.97
Rb	**0.92**	0.35	0.16	0.99
Pr	**0.90**	0.38	0.14	0.98
Nd	**0.90**	**0.40**	0.13	0.98
La	**0.89**	0.39	0.13	0.97
Sm	**0.89**	**0.42**	0.14	0.99
Gd	**0.87**	**0.46**	0.14	0.99
Ce	**0.86**	**0.47**	0.15	0.99
Dy	**0.85**	**0.50**	0.16	0.99
Fe	**0.85**	**0.48**	0.17	0.98
Y	**0.84**	**0.50**	0.15	0.98
K	**0.84**	**0.46**	0.27	0.98
Nb	**0.82**	**0.50**	0.16	0.96
Eu	**0.80**	**0.57**	0.16	0.99
Al	**0.79**	**0.56**	0.17	0.97
Ba	**0.67**	**0.65**	0.21	0.92
Sr	**0.64**	**0.57**	**0.47**	0.96
As	0.26	**0.95**	—	0.97
Ge	0.39	**0.90**	0.12	0.97
Se	0.17	**0.89**	0.13	0.83
Ga	**0.53**	**0.83**	0.12	0.98
V	**0.53**	**0.82**	0.14	0.97
Li	**0.58**	**0.78**	0.12	0.97
Zn	0.38	**0.76**	—	0.73
Cs	**0.62**	**0.75**	0.14	0.96
Sb	**0.41**	**0.71**	0.19	0.71
Pb	**0.55**	**0.70**	0.12	0.81
U	**0.69**	**0.70**	—	0.97
Na	—	—	**0.98**	0.97
Mg	0.39	0.22	**0.88**	0.98
CPM	**0.55**	0.36	**0.71**	0.93
Eigenvalue	**16**	**11.2**	**3.1**	Total variance
Variance (%)	**50**	**34.9**	**9.7**	**94.7**

Therefore, it was not possible to obtain information related to the origin of one element based on its pattern with the distance to the thermoelectric complex.

FPM, CPM and elements temporal series were investigated based on the mean values of all sampling points. It was interesting to note how similar was the behavior of the elements belonging to a same group as shown in Fig. 4. During the three last days of the 2000 sampling campaign, it was observed an increase of the FPM and of the CPM with a consequent increase in the concentration of elements originated from soil (Al, Fe and Th). However, the behavior of the elements as Pb, Se and As was quite different with a sharp peak during the eighth sampling day. Two factors can be interpreted as the origin of such peaks: changes on the climatic conditions (e.g. height of the thermal inversion) or any operational procedure change of the TCJL with influence on the particulate matter emission.

In order to investigate the relationship between the elemental concentrations, and regional atmospheric aerosol, principal factor analysis was applied on each database. The Varimax rotated factor loading matrix are shown in Tables 6–9, where only factors with eigenvalues higher than 1 were retained. Only factor loadings higher than 0.1 are presented and in loadings are shown in bold have values higher than 0.4. These statistically significant factor loadings in bold were used in order to interpret the sources associated with each factor.

Four factors were identified for the fine particles (Tables 6 and 7), for the sampling periods of 1999 and

Table 9
Varimax rotated factor loading matrix—coarse particles 2000

Element	Factor 1 Soil ressuspension	Factor 2 TCJL emissions	Factor 3 Road dust	Factor 4 Sea spray	Communality
Th	**0.94**	0.13	0.16	0.11	0.94
Pr	**0.93**	0.23	0.22	0.14	0.98
Nd	**0.92**	0.25	0.24	0.14	0.98
La	**0.92**	0.26	0.22	0.14	0.98
Sm	**0.91**	0.25	0.26	0.13	0.98
Dy	**0.91**	0.17	0.32	0.13	0.99
Y	**0.91**	0.20	0.33	0.10	0.99
Nb	**0.91**	0.28	0.24	—	0.97
Gd	**0.91**	0.25	0.29	0.13	0.99
Ce	**0.91**	0.26	0.29	0.14	0.99
Al	**0.90**	0.19	0.36	—	0.98
Rb	**0.89**	**0.41**	0.13	—	0.99
Fe	**0.86**	**0.40**	0.23	0.12	0.96
Mn	**0.85**	**0.43**	0.13	0.11	0.93
K	**0.85**	**0.45**	0.16	0.17	0.97
Be	**0.84**	0.10	**0.50**	—	0.97
Eu	**0.83**	0.33	**0.42**	0.12	0.98
Ti	**0.79**	0.35	**0.41**	—	0.93
Cs	**0.76**	0.27	**0.56**	—	0.96
Li	**0.75**	0.20	**0.61**	0.12	0.99
Ga	**0.70**	0.17	**0.68**	—	0.98
U	**0.70**	—	**0.61**	0.15	0.89
CPM	**0.69**	**0.46**	0.21	0.31	0.83
Sr	**0.64**	0.39	0.31	**0.48**	0.89
Pb	0.21	**0.93**	—	—	0.91
Bi	0.19	**0.87**	0.35	−0.10	0.94
Se	0.29	**0.85**	0.31	—	0.91
Cd	0.18	**0.85**	0.25	—	0.81
Sb	0.33	**0.79**	—	—	0.74
Ba	**0.60**	**0.63**	0.31	—	0.86
Ge	**0.44**	0.24	**0.84**	—	0.96
V	**0.45**	0.32	**0.80**	0.11	0.96
As	0.22	**0.67**	**0.68**	—	0.96
Na	—	−0.20	—	**0.95**	0.94
Mg	**0.44**	0.14	0.21	**0.84**	0.96
Eigenvalue	**18.5**	**6.8**	**5.4**	**2.3**	Total variance
Variance (%)	**52.9**	**19.4**	**15.5**	**6.5**	**94.3**

2000, and they explain 89% of the data variability. In general, the communality was high for most of the elements, typically 90%, indicating that the identified factors explain most of the data variability of these elements. The only exception was black carbon during the 1999 sampling campaign. The soil ressuspension factor was defined based on the presence of elements such as Al, Fe, rare earths, U and Th. High factor loadings for K, Rb and BC were used to characterize the biomass burning component. The Na, Mg and Sr association represents the marine aerosol influence. Elements taken as coal burning tracers as As, Bi, Cd, Pb, Sb and Se were used to define the TCJL

component (Godoy et al., 2001). The biomass burning component on the fine particles during the winter 2000 campaign seems to contain also a soil contribution, represented by high factor loadings of crustal elements. In order to verify the orthogonality of these four identified factors, the factor scores were added as new variables to the data bank used. A hierarchical cluster analysis was then carried out and four clusters were obtained in both cases (Fig. 5). Each cluster contains one of the factor scores, and a similar pattern of elements as obtained in the PFA, showing consistency between the independent multivariate procedures.
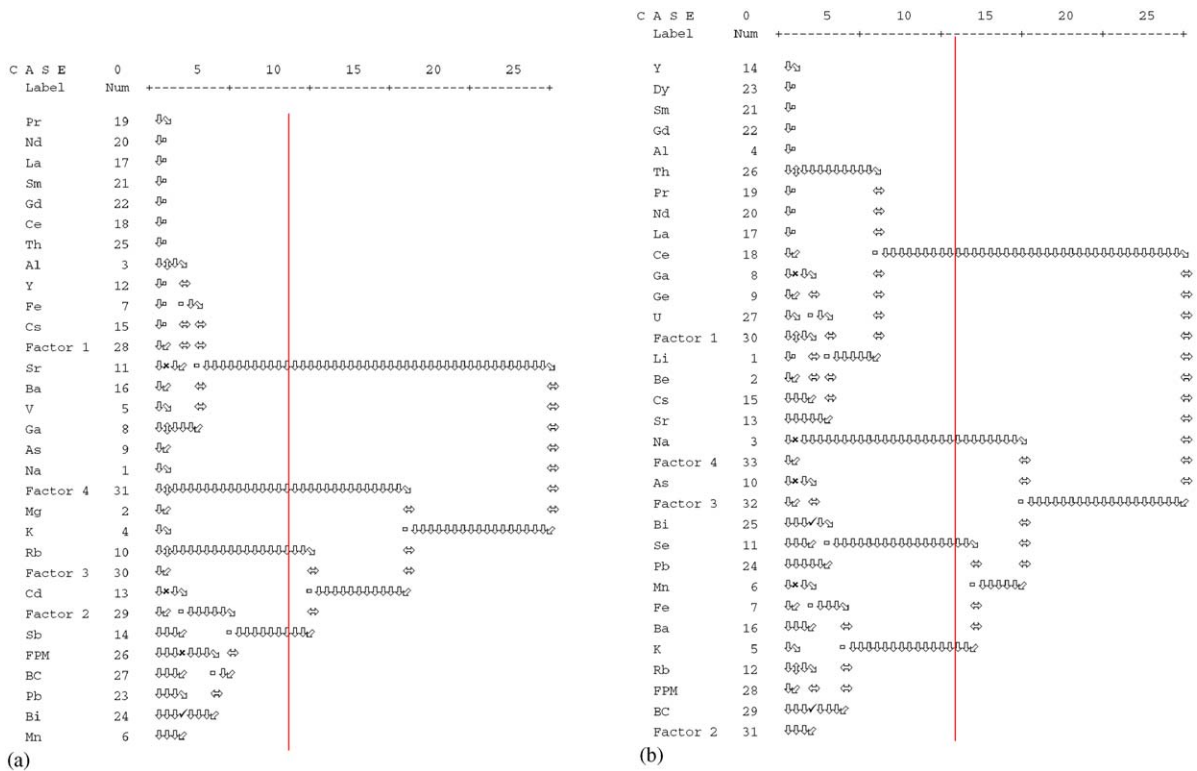
Fig. 5. Fine mode hierarchical cluster analysis dendrogram showing the distance between the elements, with the PFA factor scores included as new variables—(a) cluster results for the year 1999 sampling campaign, (b) cluster results for the year 2000 sampling campaign.

The same method was applied to the coarse particles fraction (Tables 8 and 9). More than 94% of the data variability was explained in both data sets, 1999 and 2000. However, the number of components involved was different, with 3 factors in 1999 and 4 factors in 2000. For the year 2000 it was possible to discriminated between road dust and the TCJL contribution, while for 1999 these two components were represented by one single factor. High communality indicates that the identified factors explain most of the data variability for most of the trace elements. Also, a cluster analysis procedure was performed in an identical way as for the fine particles. The same associations were obtained as those observed on the PFA, including that between road dusts and the coal burning indicators during the 1999 campaign (Fig. 6).

In order to quantify the contribution of the TCJL to the aerosol composition in this region, an absolute principal component analysis (APCA) was performed. The particulate mass distribution between the difference sources identified in the TCJL region is shown in Fig. 7. The association of the contribution of biomass burning to the year 2000 fine fraction with another source was taken as the origin of the elevate percentage attributed to the biomass (64%) when compared with the year 1999 (9%). This additional contribution was assumed to be due to secondary aerosol formation but some soil contribution may be also involved, carried out together with the secondary aerosol. Secondary aerosol seems to be also the reason for the difference of the percentage attributed to the sea spray during summer 1999 (56%) when compared to winter 2000 (1%), in particular, taking into account that sea spray is a strong source for the coarse fraction but not for the fine particles (Hien et al., 1999; Pio et al., 1996), what becomes clear for the year 2000 results. Two main sources of secondary aerosol are present in this region: one is represented by the vehicular traffic and the other by the TCJL, with its NO_x and SO_2 emissions. Based on APCA results, it is possible to say that TCJL fly ash emission contributes with about 25% of fine fraction and up to 15% of the coarse fraction. But, on the other hand, the TCJL is the major contributor of elements such as As, Bi, Cd, Pb and Se on the fine and coarse particles fractions, as shown on Fig. 8 for the year 2000.

Based on the APCA results it was possible to obtain the characteristic profile of each aerosol source involved. They were calculated by the ratio between the elemental
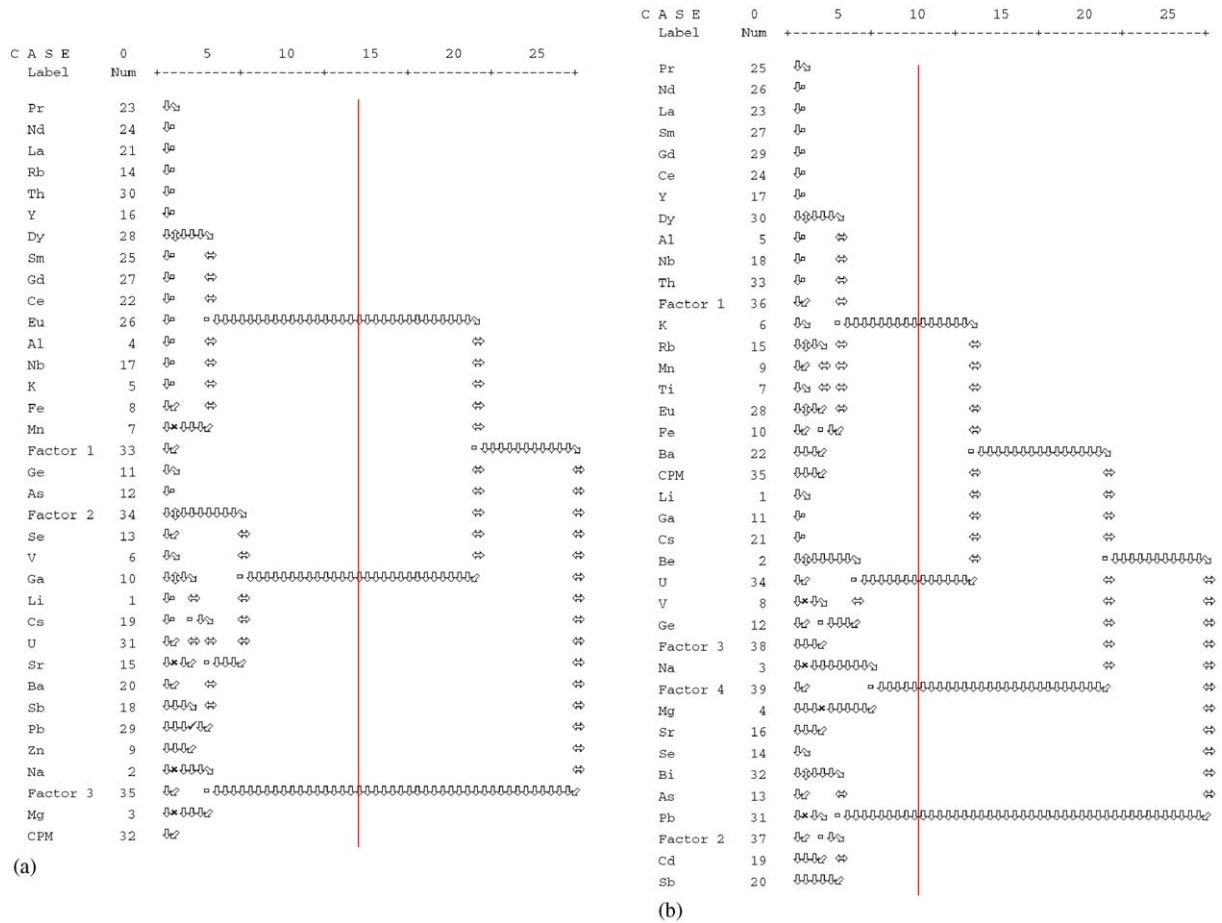
Fig. 6. Coarse mode aerosol hierarchical cluster analysis dendrogram showing the distance between the elements, with the PFA factor scores included as new variables—(a) cluster results for the year 1999 sampling campaign, (b) cluster results for the year 2000 sampling campaign.
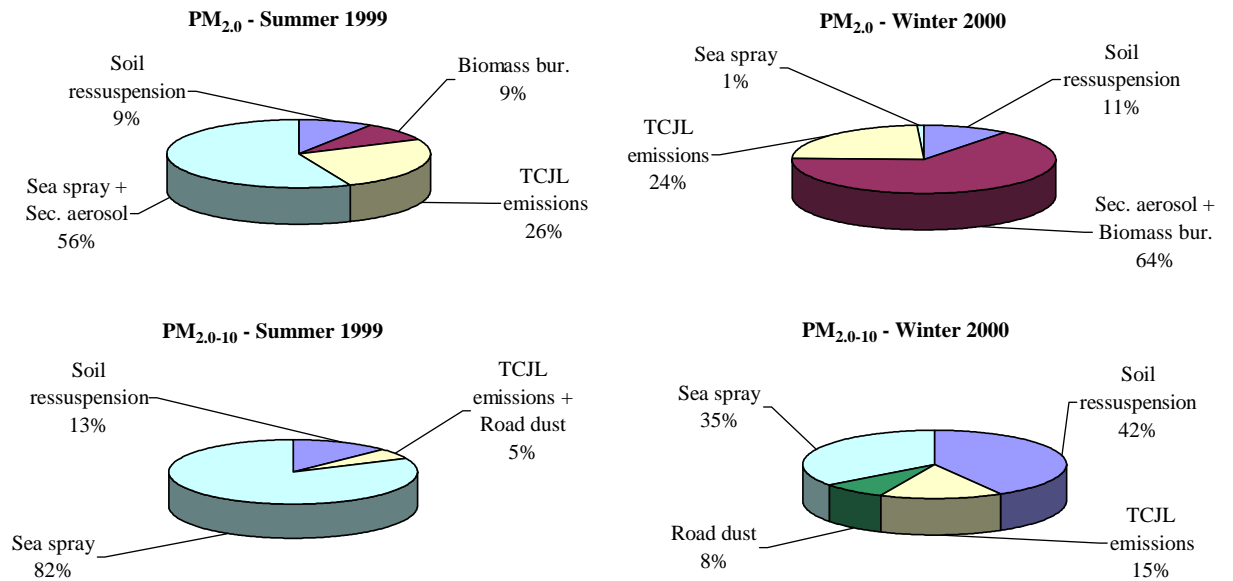

Fig. 7. Quantitative aerosol source apportionment by APCA for the fine mode and coarse mode aerosol mass concentration during both sampling campaigns.
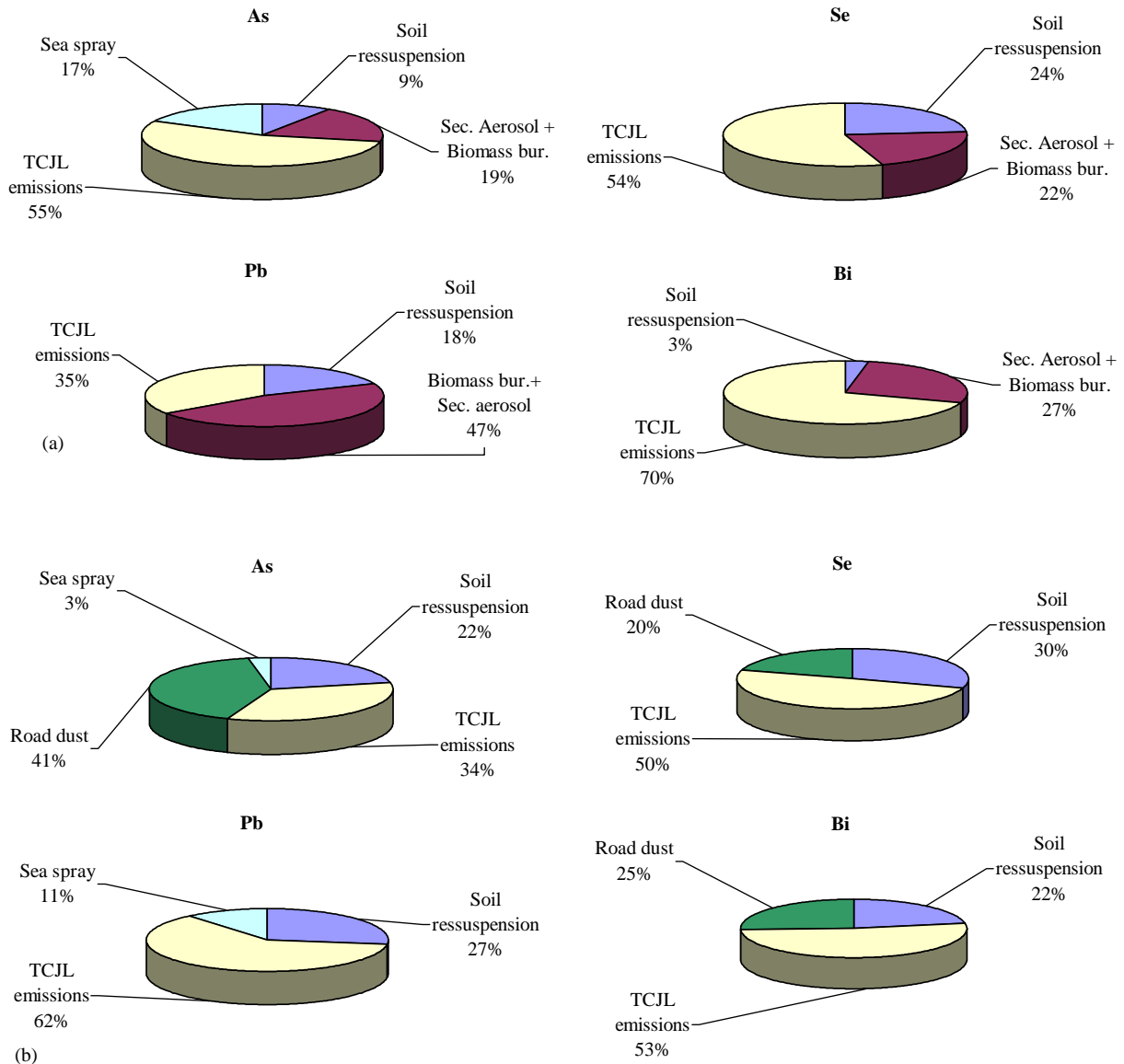
Fig. 8. Quantitative aerosol source apportionment by APCA for some elements during the winter 2000 on fine and coarse mode aerosol fractions.

and the particulate mass concentration associated to each source according the APCA results. The obtained source profiles were compared with equivalent source profiles found on the EPA Speciate 3.1 data bank, the TCJL fly ash profile (Godoy et al., 2001) and the local soil profile (Godoy et al., 2004), the results are shown on Fig. 9. In general, a good agreement is observed but the local soil profile presents lower values that those calculated based on the APCA results. On the other hand, lower results are expected since the local soil results include coarse and fine soil particles on the

(0–5) cm soil layer while the aerosol only the fine soil particles found on the top surface.

4. Conclusions

In this study it was possible to observe that using advanced trace element analysis capable to measure a large number of elements with excellent detection limits coupled with different multivariate statistical analysis can provide good quantitative information on aerosol
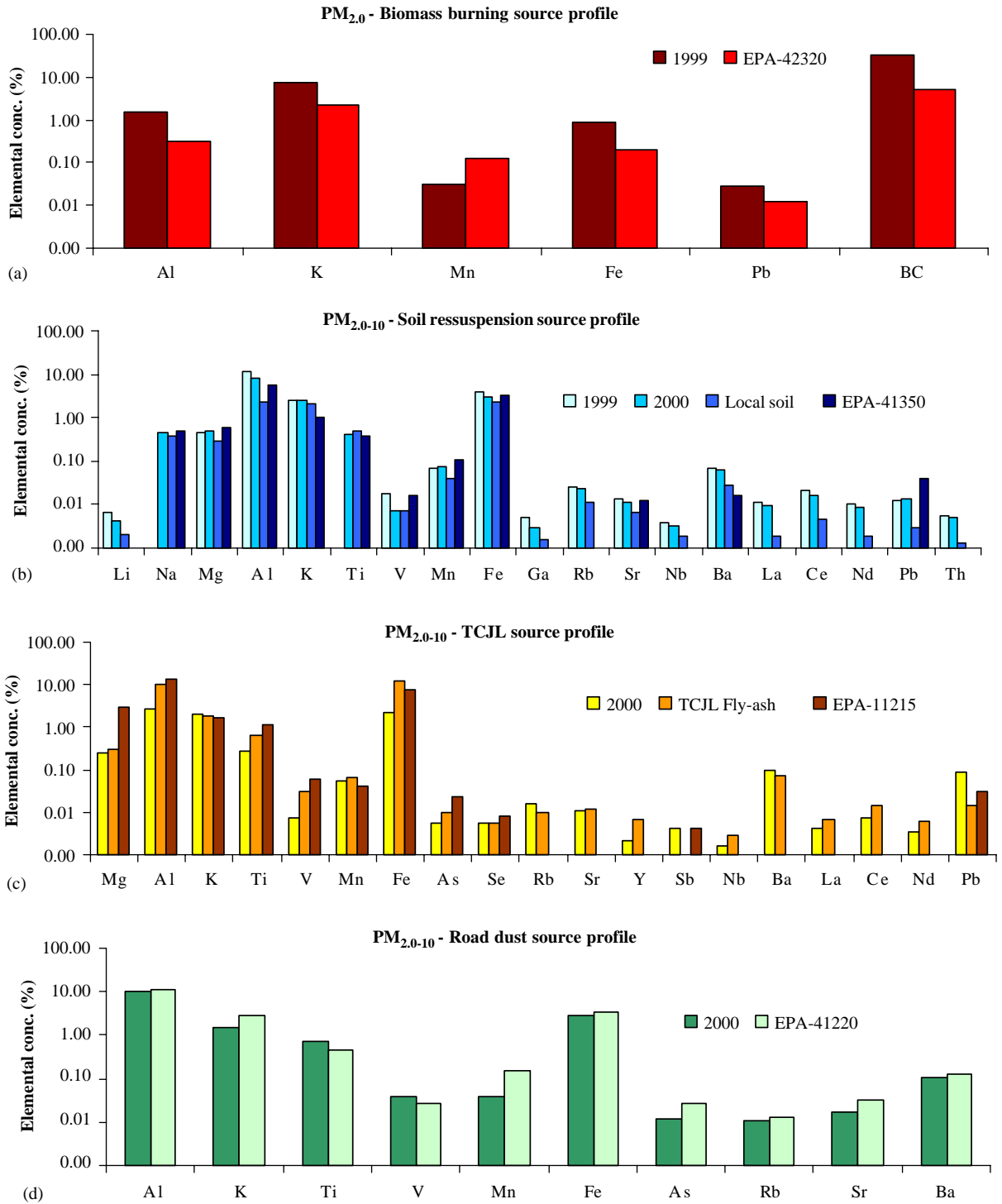
Fig. 9. Elemental source profiles calculated based on the APCA results; the EPA references represent the Speciate 3.1 source profile utilized: (a) biomass burning on fine mode particles; (b) soil ressuspension on coarse mode particles; (c) TCJL emission on coarse mode particles; (d) road dust on coarse mode particles.

sources in industrial complexes. The combined use of cluster and factor analysis with a data base of 42 elements plus BC and aerosol mass is a powerful tool for aerosol source apportionment. During the sampling periods, no violations of the Brazilian PM_{10} and the EPA $PM_{2.5}$ standards have been observed. Based on receptors models, it was identified and quantified the TCJL contribution to the fine and coarse particle concentration, as 25% and 15%, respectively. This is a significant impact based on a single source and has important effects in the regional air quality. In addition, the emission from the TCJL is the main source of elements such as As, Bi, Cd, Pb, Sb and Se in both aerosol fractions, ranging from 34% up to 83% in mass. Based on absolute principal component analysis, source profiles were calculated. These profiles were compared with those observed on the EPA Speciate 3.1 data bank and a good similarity was observed. The ICP-MS analysis of trace elements in aerosols has proven to be reliable ad feasible for relatively large number of samples.

Brazil will expand significantly the use of fossil fuels for growing energy demand, since hydroelectric power is almost fully explored. The results from this study shows that the regional impact could be significant in terms of air pollution and that the best possible technology to reduce emissions is very welcome from the environmental point of view.

Acknowledgments

References

Artaxo, P., Oyola, P., Martinez, R., 1999. Aerosol composition and source apportionment in Santiago de Chile. Nuclear Instruments and Methods in Physics Research B 150, 409–416.

Castanho, A.D., 1999. Determinação Quantitativa de Fontes de Material Particulado na Atmosfera da Cidade de São Paulo. Master Thesis, Institute of Physics, Universidade de São Paulo.

Chan, Y.C., Simpson, R.W., McTainsh, G.H., Vowles, P.D., Cohen, D.D., Aailey, G.M., 1999. Source apportionment of $PM_{2.5}$ and PM_{10} at regionally representative locations during SJVAQS/AUSPEX. Atmospheric Environment 30, 2079–2112.

Godoy, M.L., 2001. Avaliação do Impacto Ambiental Causado pela Emissão Atmosférica de Elementos Traço pelo Complexo Termelétrico Jorge Lacerda, Capivari de Baixo, SC. Ph.D Thesis, Chemistry Department, Pontifícia Universidade Católica do Rio de Janeiro, 153p.

Godoy, M.L., Godoy, J.M., Roldão, L.A., 2001. Determination of trace elements in coal and coal ash samples by ICP-MS. Atomic Spectroscopy 21, 235–242.

Godoy, M.L., Godoy, J.M., Roldão, L.A., Conti, L.F., 2004. Application of multivariate statistical analysis to superficial soils around a coal burning power plant. Journal of the Brazilian Chemical Society 15, 122–130.

Harrison, R.M., Smith, D.J., Pio, C.A., Castro, L.M., 1997. Comparative receptor modelling study of airbone particulate pollutants in Birmingham (United Kingdom), Coimbra (Portugal) and Lahore (Pakistan). Atmospheric Environment 31, 3309–3321.

Hien, P.D., Binh, N.T., Truong, Y., Ngo, N.T., 1999. Temporal variation of source impacts at the receptor, in Ho Chi Minh City, Vietnam. Atmospheric Environment 33, 3133–3142.

Hien, P.D., Binh, N.T., Troung, Y., Ngo, N.T., Sieu, L.N., 2001. Comparative receptor modelling study of TSP, PM_2 and PM_{2-10} in Ho Chi Minh City. Atmospheric Environment 35, 2669–2678.

Hopke, P.K., 1999. An introduction to source receptor modeling. In: Elemental Analysis of Airborne Particles. Gordon and Breach Science Publishers, Amsterdam, pp. 273–315.

Hopke, P.K., Xie, Y., Raunrmaa, T., Biegalski, S., Landsberger, S., Maenhaut, W., Artaxo, P., Cohen, D., 1997. Characterization of the gent stacked filter UNIT PM_{10} sampler. Aerosol Science and Technology 27, 726–735.

Horton, J.H., Dorsett, R.S., Cooper, R.E., 1977. Trace Elements in the Terrestirial Environment of a Coal Fired Powerhouse. DP-175, UC-11.

Japan International Cooperation Agency (JICA), 1997. The study on evaluation of environmental quality in regions under influence of coal steam power plants in the Federal Republic of Brazil, Final Report, Tokyo, Japan.

Johansson, T., van Grieken, R., Winchester, J., 1974. Interpretation of Aerosol Trace Metal Particle Size Distribution. In: Conference on Nuclear Methods in Environmental Research, Columbia, USA.

Johnson, R.A., Wichern, D.W., 1998. Applied Multivariate Statistical Analysis, fourth ed. Prentice-Hall, New Jersey.

Klein, D.H., Andren, A.W., Carter, J.A., Emery, J.F., Feldman, C., Fulkerson, W., Lyon, W.S., Ogl, J.C., Talmi, Y., Hook, R.I., Bolton, N., 1975. Pathways of thirty-seven trace elements through coal-fired power plant. Environmental Science and Technology 9, 973–979.

Legendre, P., Legendre, L., 1998. Numerical Ecology: Developments in Environmental Modelling 20, second ed. Elsevier, New York.

Lindberg, S.E., Andren, A.W., Raridon, R.J., Fulkerson, W., 1975. Mass balance of trace elements in walker branch watershed: relation to coal-fired steam plants. Environmental Health Perspectives 12, 9–18.

Maenhaut, W., François, F., Cafmeyer, J., 1993. The "GENT" stacked filter unit (SFU) sampler for the collection of atmospheric aerosols in two size fractions: description

and instructions for installation and use. Report No. NAHRES-19, International Atomic Energy Agency, Vienna, p. 249–263.

Pio, C., Castro, L.M., Cerqueira, M.A., Santos, I.M., Belchior, F., Salgueiro, M.L., 1996. Source assessment of particulate air pollutants measured at the Southwest European coast. Atmospheric Environment 30 3309, 3320.

Swietlicki, E., Puri, S., Hansson, H.C., 1996. Urban air pollution source apportionment using a combination of aerosol and gas monitoring techniques. Atmospheric Environment 30, 2795–2809.

Zoller, W., Gladney, E., Duce, R., 1974. Atmospheric concentrations and sources of trace metals at the South Pole. Science 183, 198.